Ultrasound Obstet Gynecol 2022; **60**: 28–41
Published online in Wiley Online Library (wileyonlinelibrary.com). **DOI:** 10.1002/uog.24816

State-of-the-Art Review

Doppler evaluation of normal and abnormal placenta

E. HERNANDEZ-ANDRADE[1]*, E. S. HUNTLEY[1], M. F. BARTAL[1], E. E. SOTO-TORRES[1], D. TIROSH[2], S. JAIMAN[3] and A. JOHNSON[1]

[1]*Department of Obstetrics and Gynecology and Reproductive Sciences, McGovern Medical School, University of Texas, Health Science Center at Houston (UTHealth), Houston, TX, USA;* [2]*Department of Obstetrics and Gynecology, Soroka University Medical Center, Faculty of Health Sciences, Ben-Gurion University of the Negev, Beer Sheva, Israel;* [3]*Department of Obstetrics and Gynecology Wayne State University, Detroit, MI, USA*
**Correspondence.*
(e-mail: Edgar.A.HernandezAndrade@uth.tmc.edu)

ABSTRACT

Doppler techniques are needed for the evaluation of the intraplacental circulation and can be of great value in the diagnosis of placental anomalies. Highly sensitive Doppler techniques can differentiate between the maternal (spiral arteries) and fetal (intraplacental branches of the umbilical artery) components of the placental circulation and assist in the evaluation of the placental functional units. A reduced number of placental functional units can be associated with obstetric complications, such as fetal growth restriction. Doppler techniques can also provide information on decidual vessels and blood movement. Abnormal decidual circulation increases the risk of placenta accreta.

Doppler evaluation of the placenta greatly contributes to the diagnosis and clinical management of placenta accreta, vasa previa, placental infarcts, placental infarction hematoma, maternal floor infarction, massive perivillous fibrin deposition and placental tumors. However, it has a limited role in the diagnosis and clinical management of placental abruption, placental hematomas, placental mesenchymal dysplasia and mapping of placental anastomoses in monochorionic twin pregnancies. © 2021 International Society of Ultrasound in Obstetrics and Gynecology.

INTRODUCTION

The placenta is a vascular organ with an enormous capacity to accumulate blood. All vessels within the placenta are of fetal origin, whereas maternal blood moves freely around the villi. In the normal placenta, there are no maternal vessels and there is no free fetal blood; these two concepts are key when evaluating different Doppler modalities. Most studies on placental circulation have focused on the uterine arteries, representing the maternal component, and the umbilical arteries, representing the fetal component. In this Review, we describe the use of Doppler techniques for the evaluation of intraplacental blood movement and their contribution to the diagnosis and clinical management of perinatal complications.

NORMAL PLACENTAL CIRCULATION

Maternal component

Uterine blood supply

The mechanisms and dynamics of maternal blood movement into the placenta have not been described extensively. Konje *et al.*[1] used ultrasound and Doppler techniques to report uterine blood flow of 513.1 ± 127.1 mL/min at 20 weeks' gestation that increased up to 970.1 ± 193.1 mL/min at 38 weeks. The fraction distributed to the uteroplacental circulation has been estimated to be about 3.5% of the total cardiac output in early pregnancy (12 weeks' gestation) and about 16–20% at 36 weeks[2]. The unilateral arterial and venous blood flow values at 28 weeks, calculated by magnetic resonance echo planar imaging technique, have been estimated to be 203 ± 159 mL/min and 274 ± 218 mL/min, respectively[3].

Intraplacental blood flow

The placenta does not contain maternal vessels. Maternal blood is delivered by the spiral arteries in the endometrial–myometrial interface (Figure 1a). Color Doppler techniques (directional color imaging and power Doppler ultrasound) can show maternal blood entering the placenta through the maternal–placental interface in the form of 'jets' (Figure 1b). The velocity of these jets is related to the size of the spiral artery. Increased jet velocity or 'mega jet' is defined as maternal blood movement visible ≥ 10 mm distal from the maternal–placental interface or reaching the middle of the placenta (Figure 1c)[4]. The lumen size of the spiral artery and the length of the jets increase with gestation, but the peak velocity becomes reduced. Mega jets have been reported in 13% of pregnant women during the first trimester and in 87% at 33–34 weeks (Figure 1d)[4]. The presence of both mega jets and placental lakes is mainly seen in late gestation, whereas isolated mega jets are more common in early pregnancy[5]. Mega jets have been associated with trophoblast invasion reaching the basal arteries or fusion of two or more spiral arteries[4]. The distance between jets increases near the periphery of the placenta and in obstetric complications, such as a small-for-gestational-age fetus and pre-eclampsia[6].

Doppler velocimetry studies of the spiral arteries show a reduction in the pulsatility index (PI) from 0.8 in the first trimester to 0.5 in the second and third trimesters[7] and a similar reduction in the resistance index (first trimester, 0.34; second trimester, 0.28; third trimester, 0.27) (Figure 2)[8], with no changes in peak systolic velocity (PSV) (first trimester, 0.22 m/s; second trimester, 0.28 m/s; third trimester, 0.25 m/s; $P = 0.56$)[7]. Spiral artery PI has been shown to be higher in the first and second trimesters among pregnant women who developed complications (i.e. hypertensive disorders, fetal growth restriction, preterm labor, placental abruption) as compared with uncomplicated pregnancies (1.49 *vs* 0.80; $P < 0.001$)[7].

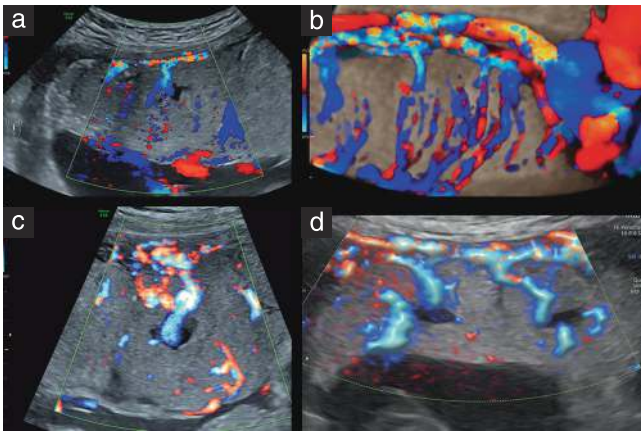

Figure 1 Color Doppler imaging of the spiral arteries. (a) Directional color Doppler image showing a spiral artery originating from a radial artery and a blood jet entering the placenta. (b) Three-dimensional color Doppler rendered image showing several blood jets originating from the spiral arteries and a rich vascular network of fetal vessels originating from the chorionic plate. (c) Mega jet reaching the middle of the placenta. (d) Blood jets from spiral arteries forming small placental lakes. Image courtesy of the Perinatology Research Branch NICHD/NIH/DHHS.

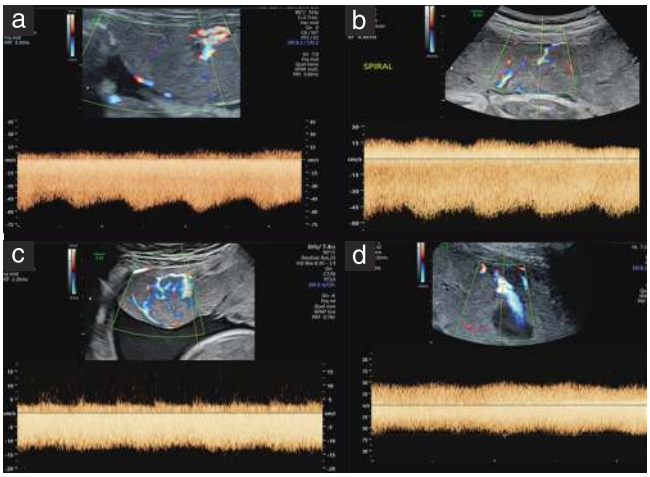

Figure 2 Spectral pulsed Doppler velocimetry of blood jets from the spiral arteries. The Doppler waveform reflects the maternal cardiac cycle and is seen mainly near the origin of the jet, where blood velocity is higher (a,b); deep in the placenta, the blood flow pattern is almost continuous and velocity is lower (c,d).

The movement of maternal blood within the placenta has been tracked using ultrasound contrast in 25 pregnant women[9]. Ultrasound contrast agents entered the placenta 25 s after injection in the maternal brachial vein and reached all placental regions 5–8 min after injection. The slow movement of blood within the placenta creates irregular hypoechoic areas communicating with different placental regions. Novel Doppler modalities enhance visualization of these hypoechoic areas, highlighting two main characteristics: (1) dynamic changes in shape and size and (2) the presence of moving particles swirling inside the hypoechoic area. Both characteristics can be identified on grayscale ultrasound, but Doppler techniques, in particular tissue color Doppler, allow better visualization of this slow blood movement than do directional color and power Doppler techniques (Figure 3). Assessment of blood movement within hypoechogenic areas might help to differentiate lakes from infarcted regions.

Decidual blood flow

The decidua plays a fundamental role in the interaction between the uterus and the placenta. Abnormal decidual development is related to early fetal loss and increases the risk of an abnormally invasive placenta[10–13]. Three layers of the decidua have been described: (1) decidua basalis, located at the site of placental insertion; (2) decidua capsularis, surrounding the gestational sac; and (3) decidua parietalis, which is not in contact with the embryo[14,15]. The three layers are separate until the fourth month of pregnancy, after which the decidua capsularis and decidua parietalis fuse and become one layer, thereby obliterating the uterine cavity[16]. After the fusion, the decidua capsularis degenerates at approximately 22–24 weeks owing to a reduced blood supply[16]. In early pregnancy, the gestational sac is implanted in the decidua, characterized by a rich vascular network. In late gestation, the decidua appears as a hypoechoic region of variable thickness

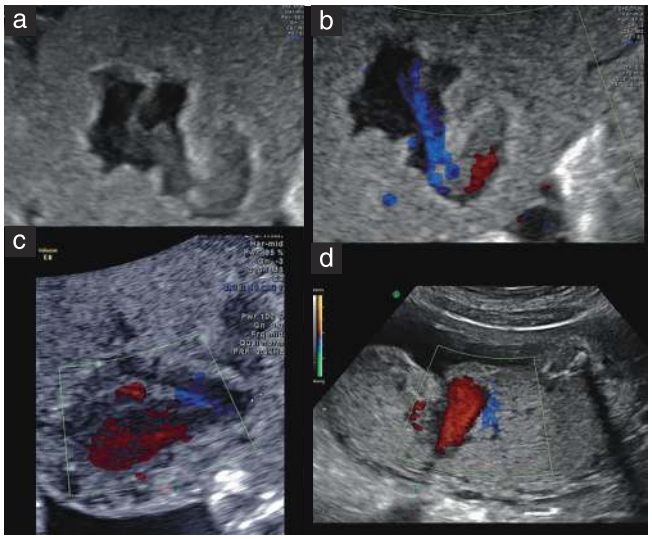

Figure 3 Grayscale ultrasound (a) and tissue color Doppler (b–d) images showing swirling blood movement within a placental lake.

located between the chorion and the uterus. This hypoechoic region has several echogenic lines reflected from the vascular walls. In late gestation, this hypoechoic area can be mistaken for an abruption; however, directional color imaging and power Doppler ultrasound show a rich maternal vascular component with very low resistance (Figure 4)[17]. Reduced or absent decidual blood flow can be associated with an abnormally invasive placenta[13]. More studies on decidual perfusion/circulation are needed.

Fetal component

Placental surface vessels

The umbilical arteries start branching at the placental insertion. Large arteries and veins are seen at the placental surface converging at the cord insertion (Figure 5). Peker *et al.*[18] applied a vascular-cast technique to evaluate the branching pattern of the umbilical artery and measure the diameter of the branches in placentae obtained from cases with uncomplicated pregnancy and delivery. They described four-order branching of the umbilical artery: (1) main branch (one per artery), located at the site of cord insertion, with a mean (± SD) diameter of 7.9 ± 0.54 mm; (2) second-order branches (4–9 branches, with a median of seven branches from the main branch), with a mean diameter ranging from 3.3 to 5.6 mm (± 0.9 mm); (3) third-order branches (three or four branches from each second-order branch), with a mean diameter ranging from 1.44 to 1.97 mm (± 0.78 mm); and (4) fourth-order branches (three or four branches from each third-order branch). Penetrating branches were seen arising from all surface branches.

Several authors have proposed evaluation of the placental surface branches for identification of women at risk of pre-eclampsia and/or fetal growth restriction[19–21]. Babic *et al.*[22] used spectral Doppler ultrasound to evaluate these branches in women with a normal pregnancy and in those with pre-eclampsia and/or fetal growth restriction at three locations: (1) at the insertion of the umbilical cord; (2) 4 cm from the insertion of the cord; and (3) in the peripheral region of the placenta (Figure 6). They found no differences in the PI or the resistance index among the three regions in normal pregnancies; however, the PI of all surface arterial branches was higher in women with pre-eclampsia and/or fetal growth restriction than in women with uncomplicated pregnancies[22]. Using a vascular-cast technique, Peker *et al.*[18] showed no significant differences in the diameter of primary and secondary branches or the number of cotyledons in placentae from normal and pre-eclamptic women.

Intraplacental branches

There is no defined nomenclature for the intraplacental (penetrating) branches of the umbilical artery. Major

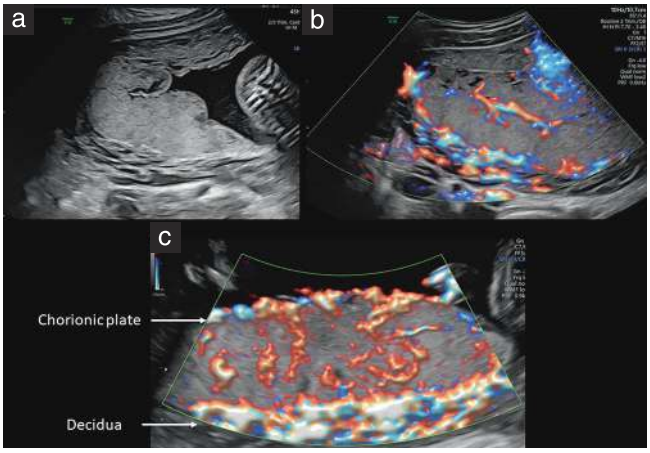

Figure 4 Grayscale (a) and directional power Doppler (b,c) images showing retroplacental space occupied by the decidua with multiple echogenic lines (a,b) and active blood movement (b), and posterior placenta with a rich vascular component in the decidua and chorionic plate (c).

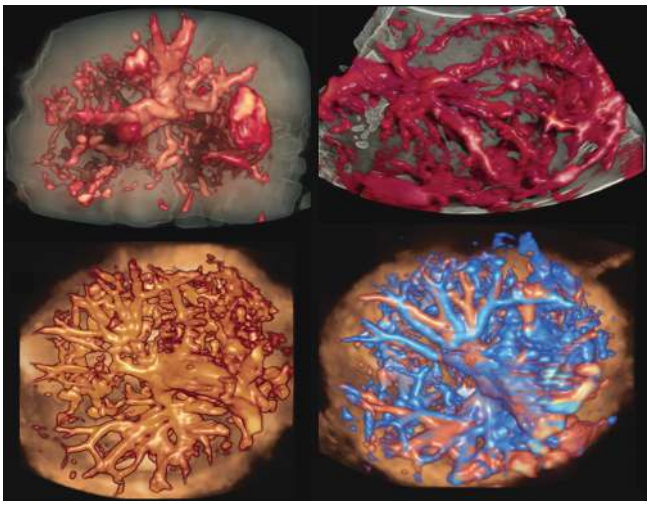

Figure 5 Three-dimensional power Doppler ultrasound rendered images of the chorionic plate, showing insertion and branching of the umbilical cord vessels.

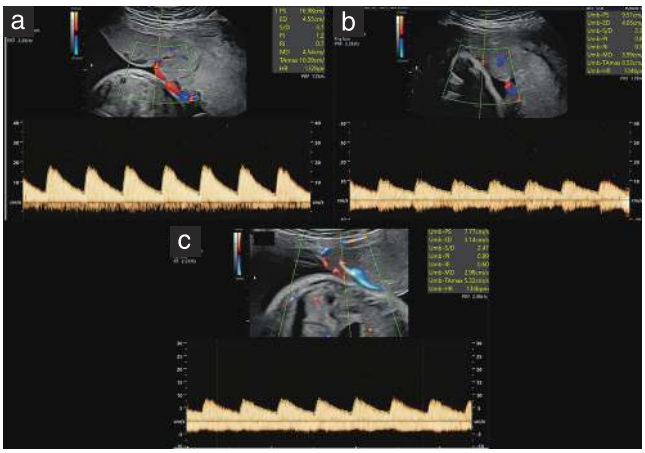

Figure 6 Spectral pulsed Doppler velocimetry of the placental surface branches of the umbilical arteries obtained at the site of cord insertion (a), between the cord insertion and placental edge (b) and near the edge of the placenta (c). There are no significant changes in pulsatility index and blood velocity as the artery approaches the placental edge.

branches immediately spread over the chorionic plate and become smaller as they penetrate into the placental parenchyma (Figure 7). All Doppler color modalities can be used to visualize these branches, but power Doppler ultrasound is the only technique that provides semi-quantitative estimation of placental blood perfusion[23]. Spectral Doppler imaging shows a pulsatile waveform with a high diastolic component throughout the complete trajectory of the branches, reflecting low vascular resistance (Figure 8). Mu *et al.*[19] proposed nomenclature of four-order branching and subsequently obtained spectral Doppler measurements approximately 5 mm distal from the origin of each branch. The authors reported a reduction in the PI and an increase in PSV in all branches with advancing gestation. Pregnancies with a growth-restricted fetus showed similar PI values in all intraplacental branches, but fewer second-, third- and fourth-order branches than did placentae in normal pregnancies.

In a study by Higgins *et al.*[24] women with reduced fetal movement in the third trimester of pregnancy were evaluated using Doppler velocimetry of the umbilical artery in the umbilical cord, the chorionic plate and the intraplacental region. The authors found a significant reduction in PI in the three sites and suggested that increased placental villous vascularity may be associated with lower impedance in all intraplacental branches.

Placental functional unit

Intraplacental branches of the umbilical artery create a rich vascular bed around maternal blood jets and placental lakes. The placental functional unit has been described previously as a placental cotyledon. Research on placental physiology is usually done after delivery using a perfused cotyledon model, in which cannulae are inserted into the chorionic plate artery and vein and into the intervillous space to investigate diffusion, perfusion and transport of metabolites[25–28]. The number of cotyledons or functional units in the normal placenta has been reported to range from 10 to 40. Mu *et al.*[19] described 22 ± 4 placental functional units at 27–29 weeks and 25 ± 4 at 36–38 weeks in normal pregnancy. The placental functional unit develops with advancing gestation. It can be evaluated using directional, power or tissue color Doppler techniques. Novel Doppler techniques, such as HDFlow® and HQSlowflow® (GE Healthcare, Zipf, Austria), Superb Microvascular Imaging® (Toshiba Medical Systems Corp., Tokyo, Japan) and MV flow® (Samsung Medison Co., Seoul, South Korea), may improve visualization of the placental functional unit (Figure 9)[29,30]. These techniques are extremely sensitive

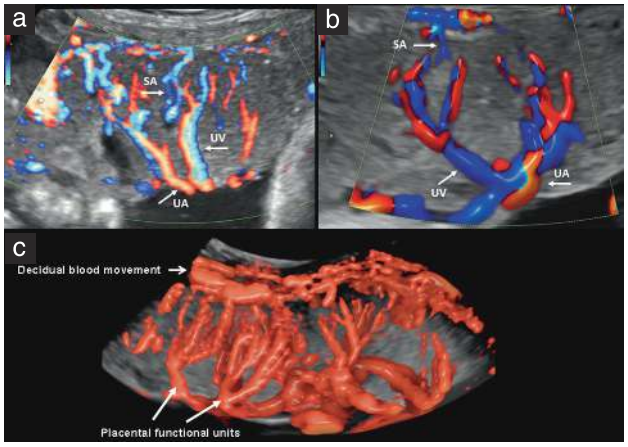

Figure 7 (a) Directional power Doppler of the intraplacental branches of the umbilical artery and vein from the chorionic plate and blood jets from the spiral arteries. (b) Three-dimensional (3D) color Doppler rendered image of the intraplacental branching of the umbilical arteries and vein. (c) 3D power Doppler rendered image showing branching and ramification of intraplacental vessels, placental functional units and decidual blood movement. SA, spiral artery; UA, umbilical artery; UV, umbilical vein.

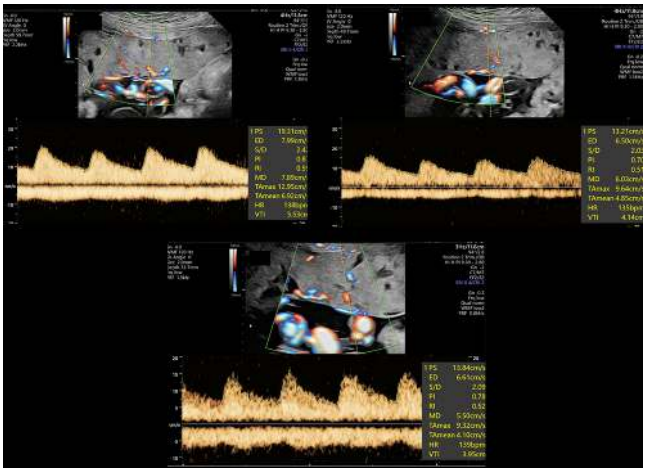

Figure 8 Spectral pulsed Doppler velocimetry of intraplacental arteries and veins. Note that veins run together with arteries. Low vascular resistance is seen in all branches. Arterial peak systolic velocities decrease as the branches get closer to the maternal uterine wall. Oscillations in the vein Doppler spectrum are reflections from arterial pulsations.

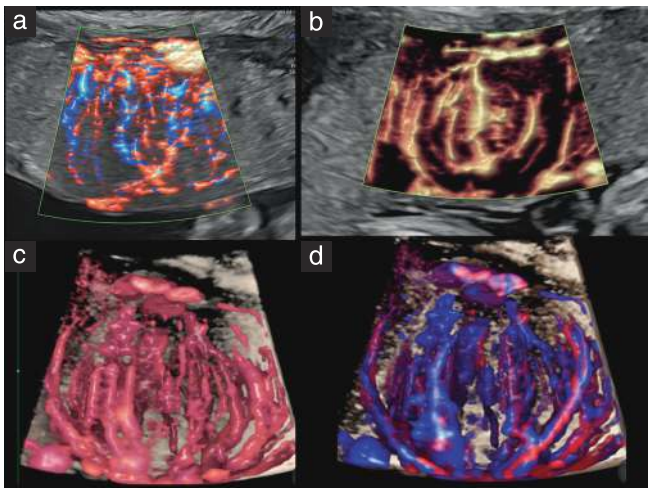

Figure 9 Directional color power Doppler (a), HQSlowflow® (b), three-dimensional rendered power Doppler (c) and directional power Doppler (d) images showing a rich network of fetal vessels surrounding a blood jet from a spiral artery. Image courtesy of the Perinatology Research Branch NICHD/NIH/DHHS.

to motion, and factors such as maternal breathing, fetal movements and uterine contractions can affect the signal. The value of these new Doppler techniques in the qualitative and quantitative assessment of the placental functional unit should be explored further[31].

CLINICAL CONDITIONS IN WHICH DOPPLER TECHNIQUES GREATLY CONTRIBUTE TO DIAGNOSIS AND MANAGEMENT (Table 1)

Doppler techniques can be of great value in the diagnosis and management of abnormally invasive placenta, vasa previa, placental lakes, placental infarcts, placental infarction hematoma, massive perivillous fibrin deposition/maternal floor infarction (MPFD/MFI) and placental tumors.

Abnormally invasive placenta/placenta accreta spectrum

Nearly 95% of placenta accreta spectrum cases can be detected on grayscale ultrasound and color Doppler modalities[32–41]. Differences in detection rate are mainly related to placental position in the uterus[42]. Anterior placenta previa in women with a history of previous Cesarean section significantly increases the risk of placenta accreta[43]. Therefore, a detailed ultrasound evaluation including Doppler modalities should be performed. The best ultrasound signs for the prediction of placenta accreta are placental lacunae, loss of the placenta–myometrium interface and dilated bulging vessels in the uterus–bladder interface (Figure 10)[44]. Placental lacunae are defined as parallel, irregular hypoechoic, elongated areas extending through the placental parenchyma near the site of abnormal placental implantation with high blood velocity and a non-pulsatile Doppler pattern[38]. Zhang *et al.*[45] reported that women with an abnormally invasive placenta had significantly higher PSV in the intraplacental vessels than did those without an abnormally invasive placenta (56.1 ± 16.7 *vs* 33.7 ± 8.1 cm/s; $P < 0.0001$). The authors reported that PSV ≥ 41 cm/s had a diagnostic sensitivity of 87%, specificity of 78%, positive predictive value of 75% and negative predictive value of 89% for abnormally invasive placenta. PSV ≥ 49 cm/s was observed only in women with placenta increta or percreta.

Bulging vessels through the myometrium and bladder wall can be visualized using three-dimensional (3D) color Doppler[46]. Collins *et al.*[47] applied 3D power Doppler

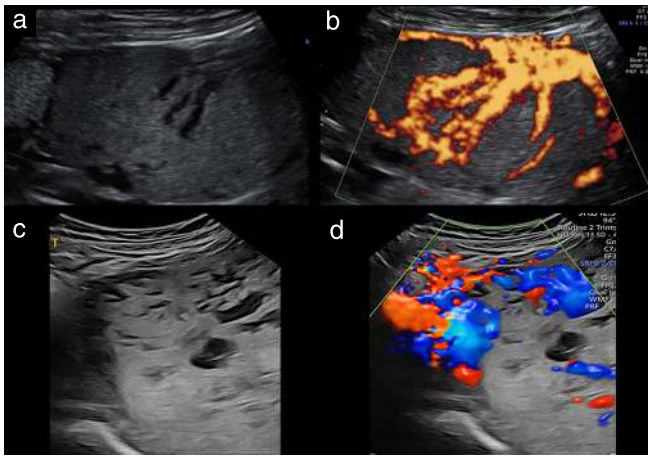

Figure 10 Two dimensional grayscale (a,c), power Doppler (b) and color Doppler (d) images in two cases of placenta accreta, showing placental lacunae and increased vascularization (a,c) and atypical, increased blood flow pattern (b,d). Images (a) and (b) courtesy of the Perinatology Research Branch NICHD/NIH/DHHS.

Table 1 Clinical conditions in which Doppler techniques greatly contribute to diagnosis and management

Condition	*Doppler findings*	*Contribution*
Abnormally invasive placenta/PAS	Placental lacunae, increased vascularization, high intraplacental blood velocity, bulging vessels, chorionic and bladder bridging vessels (rail sign), increased blood perfusion	Important: Doppler findings are key for diagnosis and clinical management
Vasa previa	Vascular structure near or over internal cervical os, venous or fetal arterial Doppler waveform	Important: diagnosis is based on Doppler findings
Placental lake	Attached to spiral artery, blood movement within lake, dynamic change in shape and size	Important: lakes are generally benign; extended lakes may affect fetal growth
Placental infarct	Not attached to spiral artery, no blood movement within or around hypoechoic area, no dynamic changes in shape and size	Important: Doppler evaluation can differentiate between placental lake and infarct
Placental infarction hematoma	Large area with mixed echogenicity, reduced blood movement within and around lesion	Complementary: diagnosis is based mainly on 2D images; Doppler techniques can contribute
MPFD/MFI	Enlarged placenta with multiple small cystic areas without blood flow, large cystic areas with characteristics similar to those of infarction	Important: lack of blood movement is key for differentiation from placental mesenchymal dysplasia
Placental tumors	Chorioangioma: increased vascularization within and around tumor; teratoma: reduced vascularization compared with surrounding placental tissue; choriocarcinoma: increased vascularization similar to that of chorioangioma	Complementary: Doppler techniques may help differentiate between vascular and solid tumors

2D, two-dimensional; MPFD/MFI, massive perivillous fibrin deposition/maternal floor infarction; PAS, placenta accreta spectrum.

ultrasound to delineate the vascular area near the site of abnormally invasive placenta. The authors called it an 'area of vascular confluence', which may represent an arteriovenous fistula. The area of confluence was significantly greater in women with an abnormally invasive placenta compared with those with normal placental implantation (median, 44.2 cm^2 (interquartile range (IQR), 31.4–61.7 cm^2) *vs* 4.5 cm^2 (IQR, 2.9–6.6 cm^2); $P = 0.001$). The area was even greater in women with an abnormally invasive placenta requiring hysterectomy, with a significant difference compared to those who underwent placental removal without hysterectomy (median, 46.6 cm^2 (IQR, 37.2–72.6 cm^2) *vs* 28.4 cm^2 (IQR, 21.9–33.6 cm^2); $P = 0.005$). The authors concluded that the area of confluence may predict not only an abnormally invasive placenta but also the severity of placental invasion. Haidar *et al.*[48] estimated 3D power Doppler perfusion indices in 50 women at risk of placenta accreta. They reported a significantly higher vascularization index (VI) in women with placenta accreta ($n = 23$) than in women with a non-invasive placenta ($n = 27$) (32.8 ± 7.4 *vs* 12 ± 4.1). Prediction analysis showed that VI had 95.1% sensitivity and 91.3% specificity for placenta accreta. The authors reported that VI ≥ 31 predicted severe blood loss and need for blood transfusion with 100% sensitivity, 90.3% specificity and a positive likelihood ratio of 10.0 in patients with placenta increta or percreta corroborated by histopathology.

Shih *et al.*[49] reported the development of two parallel circulations, one in the bladder mucosa and the other in the myometrium, with branching vessels across the two systems, termed the 'rail sign' (Figure 11). This sign was observed in 54.1% (72/133) of women with placenta accreta, mainly after 38 weeks' gestation, and was associated with greater blood loss during surgery, earlier gestational age at delivery and longer hospital stay. Color Doppler imaging has been shown to contribute further to the diagnosis of placenta percreta and increta and estimation of the risk of major postpartum hemorrhage by visualization of cervical lakes and increased vascularity in the lower uterine segment extending to the parametrial region[50,51].

Vasa previa

Vasa previa is defined as at least one abnormal fetal vessel outside the placenta, running below the amniotic membranes in proximity to the internal cervical os (Figure 12). The risk of fetal hemorrhage due to rupture of membranes in these cases is very high. The importance of antenatal diagnosis has been highlighted by Zhang *et al.*[52], showing that women with vasa previa without a prenatal diagnosis had a 25-fold increased risk of neonatal mortality and a 50-fold increased risk of neonatal hypoxic morbidity than did women with prenatally diagnosed vasa previa. Diagnosis of vasa previa is done by direct visualization of the abnormal vessel(s) using transvaginal ultrasound and Doppler velocimetry in the sagittal or transverse view of the cervix[53,54]. Directional color imaging shows either one vessel (artery or vein) or two vessels (artery and vein), and spectral Doppler demonstrates blood movement with a venous or arterial waveform of fetal origin. Directional color imaging also contributes to the characterization of velamentous cord insertion and tracing of vessels connecting to an extraplacental lobe[55]. When three vessels are seen, it is most likely a funic presentation of a normal umbilical cord. Detailed screening for vasa previa should be performed in women with an extraplacental lobe and those with a marginal and velamentous insertion of the umbilical cord. Serial ultrasound can be helpful to corroborate changes in the location of the vascular structure[56].

In a study of 26 830 patients, Zhang *et al.*[57] reported an incidence of vasa previa of 0.08% or 1 in 1278 pregnant women. The authors described that, among women with vasa previa ($n = 21$), 15 (71.4%) underwent elective Cesarean section at a median gestational age of

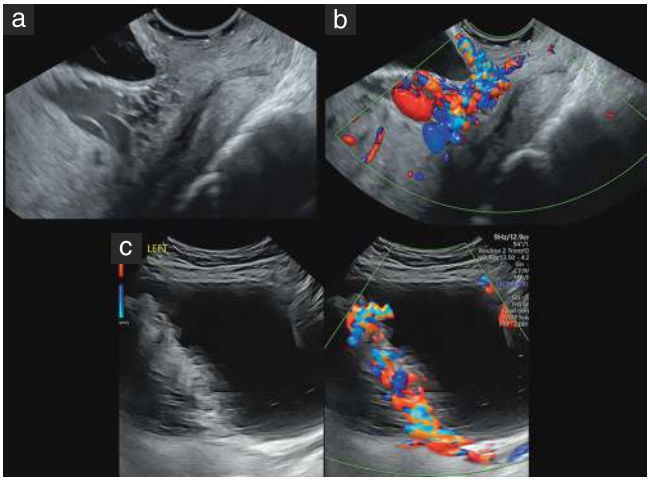

Figure 11 Transvaginal ultrasound in a case of placenta previa totalis, showing hypoechogenic areas between the lower uterine segment and cervix (a) and increased vascularization (b), suggestive of placenta accreta, and bulging vessels in the uterine–bladder interface in the lower uterine segment that create a 'rail' sign (c).

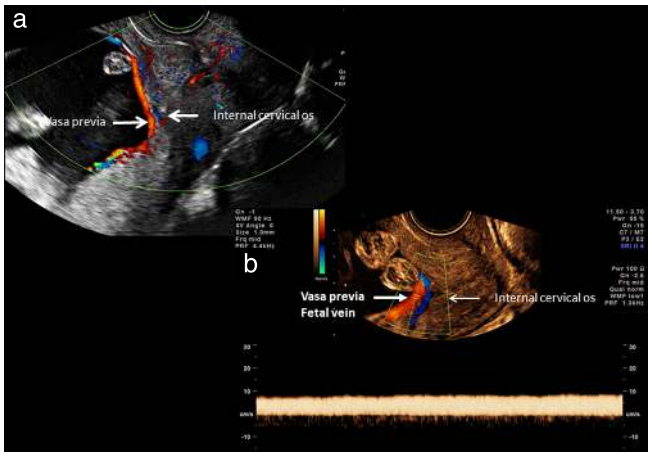

Figure 12 Color directional Doppler ultrasound images in a case of vasa previa, showing a fetal vessel running over the internal cervical os (a,b), with a continuous venous waveform seen on spectral pulsed Doppler (b). Image courtesy of the Perinatology Research Branch NICHD/NIH/DHHS.

34.2 weeks (IQR, 32.9–35.1 weeks) and six (28.6%) had spontaneous labor. Of those with spontaneous labor, five (83.3%) patients underwent emergency Cesarean section owing to an abnormal fetal heart rate and/or transvaginal bleeding. Two neonates from the spontaneous-labor group required blood transfusion because of ruptured vasa previa. These results highlight the risk associated with vasa previa even in cases diagnosed antenatally. The authors further reported that 75% of cases with vasa previa were associated with velamentous insertion of the umbilical cord and 25% with a bilobed and/or low-lying placenta at 20–22 weeks. Similar results were reported by Kulkarni *et al.*[58], who diagnosed 35 cases of vasa previa from 56 000 deliveries, with an incidence of 1/1600. In their study, 21 (63.6%) patients underwent elective Cesarean section and 12 underwent emergency Cesarean delivery owing to preterm labor, rupture of membranes or vaginal bleeding[58]. Sutera *et al.*[59] highlighted the importance of evaluating the placenta, umbilical cord and amniotic membranes during the routine ultrasound scan. These authors reported a 0.03% incidence of vasa previa and demonstrated that detailed ultrasound evaluation had a detection rate of 96.2% and specificity of 100% for the condition; 93% of women with vasa previa had a risk factor or an anomalous ultrasound finding, i.e. low-lying placenta, bilobed placenta or velamentous cord insertion.

Lo *et al.*[60] reported a case of a pregnant woman with vasa previa in which spectral Doppler showed a pulsatile pattern of maternal origin. The frequency of the Doppler signal was consistent with the maternal pulse. Examination after delivery showed an accessory lobe with five intramembranous vessels connecting to the main placenta. The vessel responsible for vasa previa was a large fetal vein. The authors concluded that the lack of Wharton's jelly and proximity to a large maternal vessel were responsible for transmission of the maternal heart rate to the fetal vein.

Vasa previa can also be found in women with normal placental location; however, this is very rare. In these cases, a detailed transabdominal scan with color Doppler can detect the communicating vessel in the lower uterine segment, thus reducing the risk of bleeding during Cesarean section[61–63].

Placental lakes and infarcts

Placental lakes are hypoechoic areas larger than 2 cm containing turbulent blood flow with swirling movement (Figure 13)[64]. The shape of the lake changes dynamically and it is surrounded by a rich network of fetal vessels. Placental lakes are mainly seen during the third trimester of pregnancy and do not appear to increase the risk of perinatal complications[65,66]; however, some authors have reported a weak association between placental lakes larger than 5 cm and fetal growth restriction[64,67].

Placental infarcts are defined as hyperechoic or echolucent avascular areas within the placenta without blood flow (Figure 14a,b). Infarcts are present in approximately 20% of uncomplicated pregnancies and 40–70% of patients with mild or severe pre-eclampsia[68,69]. Hypoechogenic areas highly suggestive of placental infarcts can be seen in 72% of fetuses with absent or reversed end-diastolic velocity in the umbilical artery[70]. Hyperechoic placental cystic lesions had 37% sensitivity for confirmed villous infarcts and a high positive predictive value for fetal death when combined with abnormal uterine artery Doppler velocimetry. Placental infarcts are related to narrowing or occlusion of the spiral arteries by a thrombus[71,72]. Susceptibility to obstruction of these maternal vessels appears to be related to defective physiological transformation of the maternal arterioles in the first trimester of pregnancy. Fitzgerald *et al.*[73] reported that 50% of well-defined rounded cystic

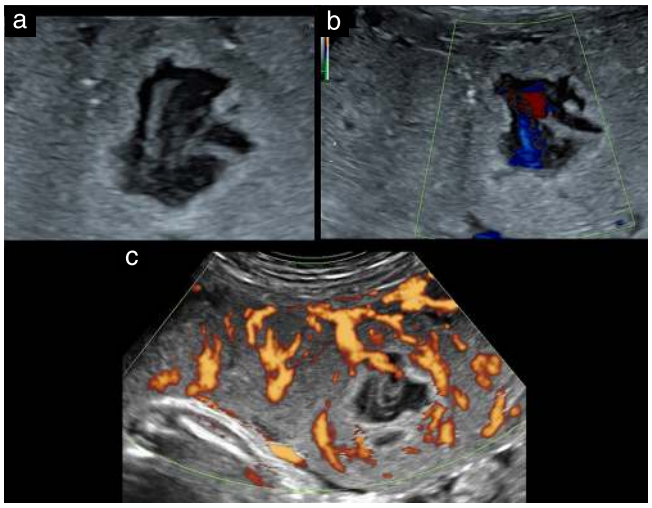

Figure 13 Grayscale (a), tissue color Doppler (b) and power Doppler (c) ultrasound images showing slow blood movement within a placental lake, with vascularization detected around the lake (c).

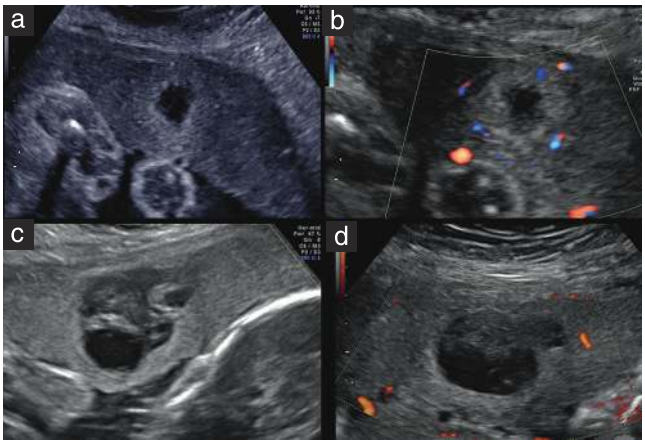

Figure 14 Sonographic features of placental infarcts (a,b) and infarction hematoma (c,d). (a,b) Placental infarct is characterized by a well-defined hypoechoic area (a) and lack of blood movement within or around it (b). (c,d) Infarction (rounded) hematoma is characterized by a large placental area with mixed echogenicity (c) and lack of blood movement within or around it (d). The echogenic rim is suggestive of infarction and the mixed echogenicity within the lesion is suggestive of hematoma.

areas were associated with placental infarcts, reflecting maternal vascular underperfusion. These patients had a higher risk for pre-eclampsia and fetal growth restriction.

Infarction hematoma, also called rounded intraplacental hematoma, is a hematoma surrounded by a rim of infarcted placental tissue (Figure 14c,d). Placental infarction hematoma occurs owing to occlusion of a spiral artery, leading to placental infarction, and subsequent recanalization of the spiral artery, thus creating a hematoma[74]. Placental infarction hematoma is strongly associated with perinatal mortality and severe fetal growth restriction[74,75]. On grayscale ultrasound, the presence of hypoechoic irregular areas with a hyperechogenic rim without blood flow is highly suggestive of placental infarction hematoma. Neville *et al.*[76] used the term 'rounded intraplacental hematoma' to refer to the same type of lesion. They described 26 women with rounded intraplacental hematoma and reported perinatal mortality in 23.1% (6/26), fetal growth restriction in 23.1% (6/26) and placental abruption in 19.2% (5/26) of cases. The authors suggested that detailed placental examination using grayscale and Doppler modalities should be performed for the diagnosis of this condition. Novel Doppler modalities, including SlowflowHD® and Superb Microvascular Imaging, might be applied to corroborate the lack of blood movement around the hypoechoic area[73,76,77]. Infarction hematoma or rounded intraplacental hematoma has a strong association with maternal vascular malperfusion lesions and decidual vasculopathy and has been linked to chronic hypertension, pre-eclampsia, gestational diabetes, fetal growth restriction, preterm delivery and fetal death[73,76].

Maternal floor infarction/massive perivillous fibrin deposition

MPFD/MFI is defined as excessive deposition of amorphous, perivillous material in the intervillous space, which comprises serum fibrin from the maternal coagulation cascade (laminated fibrin-type fibrinoid) and trophoblast-derived extracellular substance (matrix-predominant-type fibrinoid) on immunohistochemistry and microscopy[78–84]. The reported incidence of MPFD/MFI in all pregnant women is 0.09%, and it is associated with fetal death, fetal growth restriction, preterm delivery, pre-eclampsia and recurrent miscarriage[85–87]; among growth-restricted fetuses, Spinillo *et al.*[88] reported an increased rate of the condition of 11.8%. Ultrasound findings suggestive of MPFD/MFI include cystic hypoechoic areas surrounded by echogenic tissue with very low blood flow and an enlarged placenta (Figure 15). The hyperechogenic regions represent villi compressed by laminated fibrin and erythrocytes. In complicated pregnancies with echogenic lesions, Proctor *et al.*[89] reported that 60–75% of placental cystic lesions suggestive of MPFD/MFI were associated with intervillous thrombosis and 79% of women with such lesions experienced abnormal perinatal outcome, including preterm delivery, severe fetal growth restriction and perinatal death.

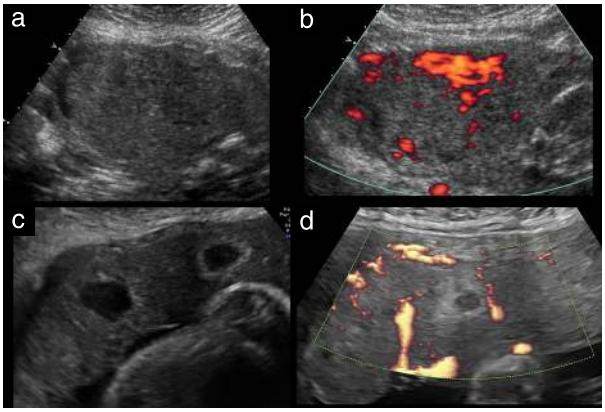

Figure 15 Sonographic features of perivillous fibrin deposition (maternal floor infarction): enlarged placenta with multiple small cystic areas (a) and minimal blood movement in the affected area (b); infarcts are also commonly seen in perivillous fibrin deposition (c,d). Images (a) and (b) courtesy of the Perinatology Research Branch NICHD/NIH/DHHS.

Placental infarction, MPFD/MFI and rounded hematoma are difficult to differentiate using ultrasound, as all these conditions share similar characteristics and can be present in the same patient. Rounded hematomas are usually larger than infarcts and MPFD/MFI can be seen as a hyperechoic area in the placenta. These three conditions are strongly associated with growth restriction and fetal demise.

Placental tumors

Non-trophoblastic placental tumor

Chorioangiomas are the most common vascular placental tumors; they are benign and identified in about 1% of all placentae[90,91]. Chorioangiomas are usually asymptomatic; however, tumors larger than 4 cm can increase the risk of fetal anemia, hydrops, polyhydramnios, growth restriction and perinatal death[92,93]. Three types of placental chorioangioma have been described: angiomatous or capillary (the most frequent), cellular and degenerative[94]. Chorioangiomas appear well-circumscribed on grayscale ultrasound, protruding from the fetal surface of the placenta near the umbilical cord insertion, with areas of hemorrhage, infarction or calcification (Figure 16). Doppler techniques show high vascularization with abundant blood flow, low resistance and the presence of arteriovenous shunts within the tumor[94–96]. The arteriovenous shunt can create cardiac overload and fetal anemia. Chorioangiomas with large vascular components are associated with a higher rate of perinatal complications than are solid chorioangiomas[94].

Teratoma is a rare tumor originating from primitive germinal cells that differentiate into multiple tissue types within the tumor. Sonographic findings include a heterogeneous cyst or a solid mass of variable size, made up of tissues with variable echogenicity. Echogenic areas

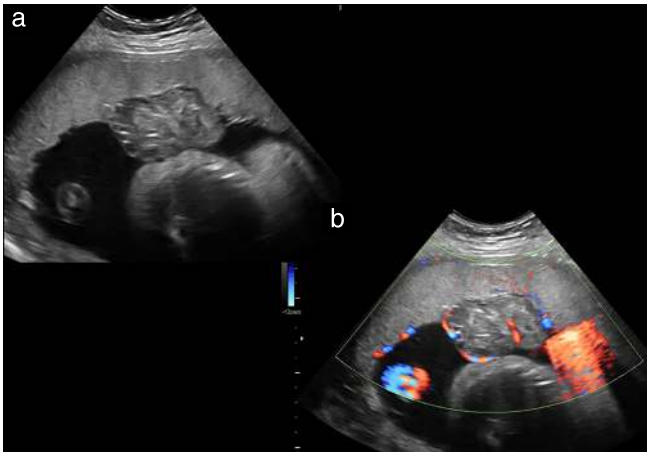

Figure 16 Grayscale (a) and color Doppler (b) ultrasound images of a chorioangioma in the placental surface, showing blood movement around and within the tumor. Image courtesy of the Perinatology Research Branch NICHD/NIH/DHHS.

suggestive of calcification or fatty tissue alternating with hypoechoic areas filled with fluid are present[97,98]. Doppler techniques show reduced vascularization as compared with the surrounding placental tissue.

Trophoblastic placental tumor

Choriocarcinoma is a highly malignant tumor originating from trophoblastic epithelial cells. Approximately 50% of cases with choriocarcinoma have a molar pregnancy, 30% result in miscarriage and 20% have an apparently normal pregnancy[99,100]. Clinical presentation includes vaginal bleeding, dyspnea and abdominal pain. The tumor frequently metastasizes to the lung and brain[101,102]. Maternal respiratory symptoms and elevated maternal serum concentrations of human chorionic gonadotropin in the presence of a placental mass confirm the diagnosis. Detailed ultrasound examination of the placenta might identify the primary tumor, typically measuring between 2.5 and 8 mm[103], with a sonographic appearance of a heterogeneous, echogenic mass and with areas of increased vascularization similar to those of a chorioangioma[104].

CLINICAL CONDITIONS IN WHICH DOPPLER TECHNIQUES HAVE LIMITED CONTRIBUTION TO DIAGNOSIS AND MANAGEMENT (Table 2)

Doppler techniques have a limited role in the diagnosis and management of placental abruption, placental hematomas and placental mesenchymal dysplasia, as well as in the mapping of placental vascular anastomoses in monochorionic twins.

Placental abruption

Ultrasound has a very low sensitivity (24%) but a relatively high positive predictive value (88%) for diagnosing placental abruption[105,106]. The main ultrasound sign is the accumulation of blood in the abruption area, with variable echogenicity depending on the time elapsed since the hemorrhage. Acute and recent hemorrhages appear as hyperechoic areas, while old hematomas are hypoechoic (Figure 17)[107]. The change from hyperechoic to hypoechoic appearance seems to occur within 2 weeks after the hemorrhage[107]. Doppler techniques show no active blood movement within the abruption area. Oyelese and Ananth[108] reported a 3.8% incidence of abruption in 7000 placentae evaluated after delivery; however, the vast majority of women in their study did not have clinical symptoms. They suggested that placental abruption should be diagnosed only when clinical symptoms are present. In a study of 27 women with suspected placental abruption due to abdominal trauma,

Table 2 Clinical conditions in which Doppler techniques have limited contribution to diagnosis and management

Condition	*Doppler findings*	*Contribution*
Placental abruption	Lack of blood movement in retroplacental space and within placenta	Low: diagnosis is mainly based on clinical symptoms; ultrasound has very low detection rate of abruption
Placental hematoma	Lack of blood movement within or around hematoma	Low: diagnosis is based on 2D ultrasound; Doppler evaluation is complementary
Placental mesenchymal dysplasia	Enlarged placenta with increased blood movement within cystic areas	Moderate: diagnosis is made based on 2D ultrasound; Doppler can help differentiation from placental floor infarction
Monochorionic twin pregnancy	Identification of placental vascular anastomoses	Low: identification of placental anastomoses using color Doppler does not contribute to diagnosis and clinical management

2D, two-dimensional.

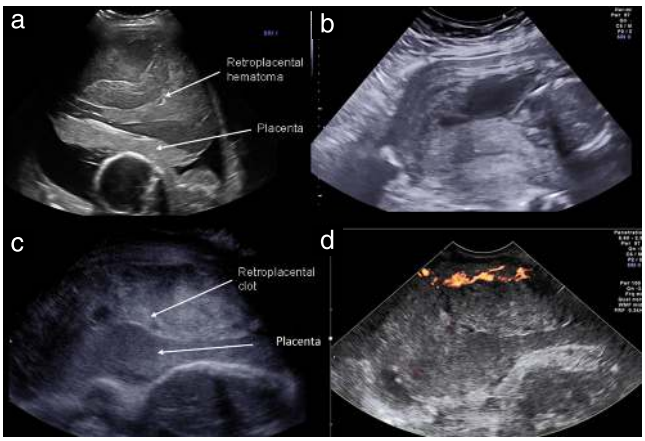

Figure 17 (a) Large retroplacental hematoma with complete placental detachment. (b) Partial abruption with marginal detachment. (c,d) Retroplacental clot with complete detachment (c) without intraplacental blood movement on color Doppler (d). Images (c) and (d) courtesy of the Perinatology Research Branch NICHD/NIH/DHHS.

histopathology evaluation of the placenta after delivery detected 10 (37.0%) cases with confirmed placental abruption, including two complete and eight partial abruptions. Ultrasound was able to reveal only cases of complete abruption (both had fetal demise at the time of ultrasound) but none of the cases of partial abruption[109]. Color Doppler techniques may contribute to clinical management of cases of placental abruption, as the presence of rich vascular placental blood flow near the site of abruption and the lack of growth of the abruption might suggest conservative management and a good prognosis[110].

Placental hematoma

There is no standard ultrasound definition of placental hematoma[111,112]. It is usually described as a hypoechoic or anechoic area located below the chorion (subchorionic), behind the basal plate (retroplacental) (Figure 18) or below the amnion (subamniotic) (Figure 19a,b)[113,114]. Massive subchorionic hematoma is termed Breus' mole (Figure 19c)[115]. These large hematomas have irregular hypoechoic areas without blood movement. They occupy approximately 50% of the placental surface and are strongly associated with adverse perinatal outcome[116–118]. Subchorionic hematoma is also known as subchorionic intervillous thrombus and is occasionally referred to as subchorionic fibrin deposition[119]. The term 'subchorionic thrombus' is preferred to the term 'subchorionic hematoma' because there are conflicting definitions in the obstetric and radiological literature, in which the term 'subchorionic hematoma' has been used for both retroplacental and retromembranous hematomas in early pregnancy[111,119,120]. No blood movement is seen inside hematomas on directional color imaging or power Doppler ultrasound; however, slow blood movement can be seen on tissue color Doppler.

Placental mesenchymal dysplasia

Placental mesenchymal dysplasia is characterized by hyperplastic mesenchymal tissue of stem villi along with findings of cystic dilatation and edema[121]. Chorionic plate and stem villous vessels show associated vascular abnormalities, including tortuosity, aneurysmal dilatation and thrombosis. The histological findings consist of mesenchymal villous hyperplasia, dilatation of the chorionic vessels, enlarged stem villi with loose connective tissue and cistern-like formations[122–124]. Mesenchymal dysplasia has a prevalence of 0.2% and is associated with overgrowth syndromes, such as Beckwith–Widemann syndrome, as well as fetal growth restriction, fetal demise and elevated levels of maternal serum alpha fetoprotein[125,126]. Differential diagnoses include molar pregnancy, chorioangioma and placental hematoma[127]. The diagnosis is made mainly in the third trimester of pregnancy based on the presence of an enlarged, thickened placenta with hypoechoic areas and increased vascularity, and elevated maternal serum alpha fetoprotein (Figure 20). Color Doppler imaging of placental mesenchymal dysplasia shows cysts with slow blood movement, which create a 'stained-glass' appearance owing to the different colors related to varying velocity and direction of blood movement within the cysts[128–130].

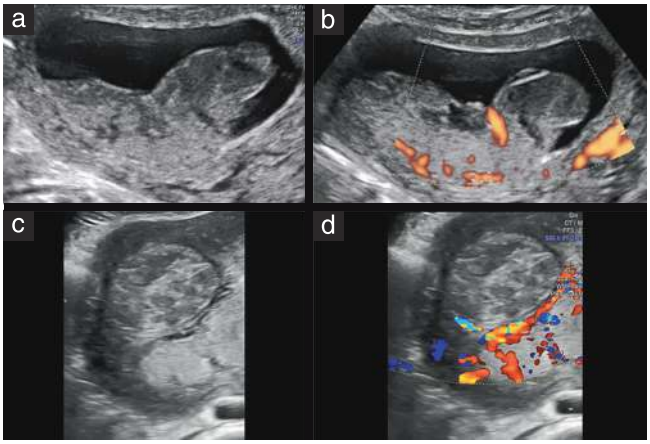

Figure 18 (a,b) Subchorionic hematomas visible below the chorionic plate, with reduced blood movement within and around the hematoma. (c,d) Retroplacental hematoma below the basal plate showing lack of blood movement within the hematoma.

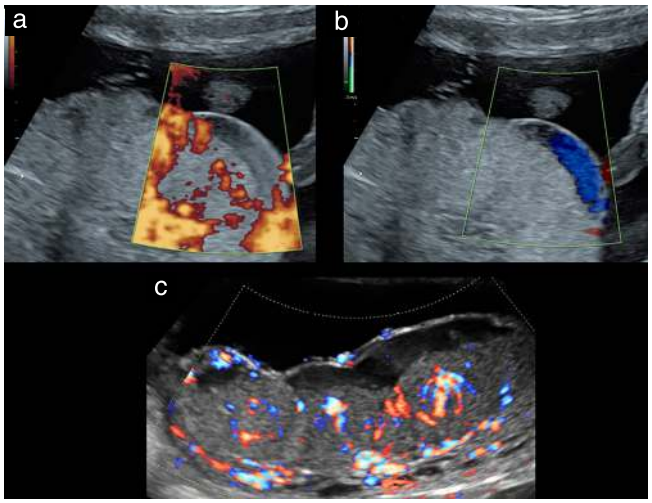

Figure 19 (a,b) Subamniotic hematoma located below the amnion and above the chorionic tissue. (a) Power Doppler ultrasound showing vessels around the hematoma. (b) Tissue color Doppler showing movements within the hematoma. (c) Massive subchorionic hematoma (Breus mole).

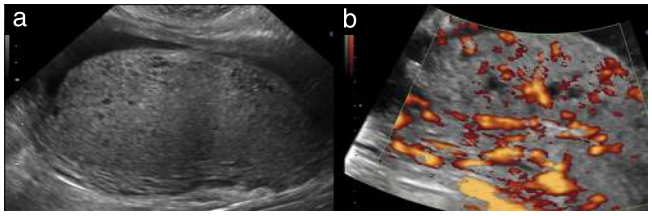

Figure 20 Sonographic features of placental mesenchymal dysplasia, including an enlarged and thickened placenta with multiple cysts (a) and slow blood movement within the cysts (b).

Mapping of placental vascular anastomoses in monochorionic twins

All monochorionic twins have placental vascular anastomoses, and an imbalance in the number and type of anastomoses is associated with perinatal complications[131]. There are two types of placental vascular anastomoses: unidirectional (arteriovenous), also called deep communications, and bidirectional (arterioarterial, venovenous), also called superficial communications[132]. Color Doppler ultrasound may allow identification of placental anastomoses. Sau *et al.*[131] studied 30 monochorionic diamniotic (MCDA) twins and identified five cases with arteriovenous placental anastomoses using color Doppler ultrasound, two (40%) of which developed twin–twin transfusion syndrome. The authors reported that visualization of vascular anastomoses was possible only in cases with an anterior placenta. Similar results were reported in a study by Fichera *et al.*[133], in which 63% of arterioarterial anastomoses were diagnosed using color Doppler imaging, mainly in anterior placentae. Spectral Doppler can be applied to identify the location of vascular collision of arterioarterial anastomosis (Figure 21)[134].

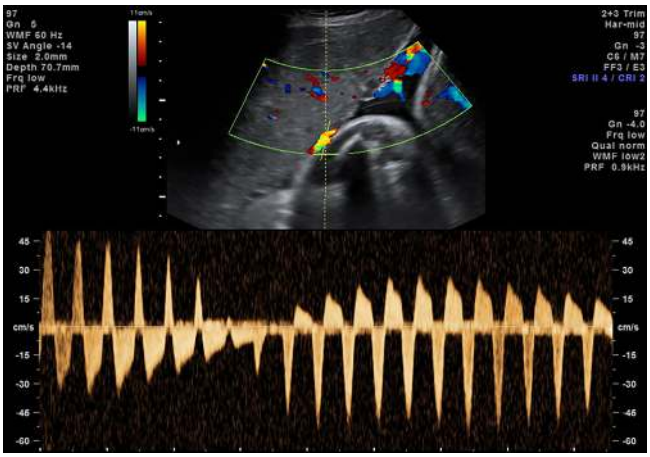

Figure 21 Spectral pulsed Doppler image showing an oscillatory pattern at the collision point of arterioarterial anastomosis in the placental surface in a monochorionic diamniotic twin pregnancy.

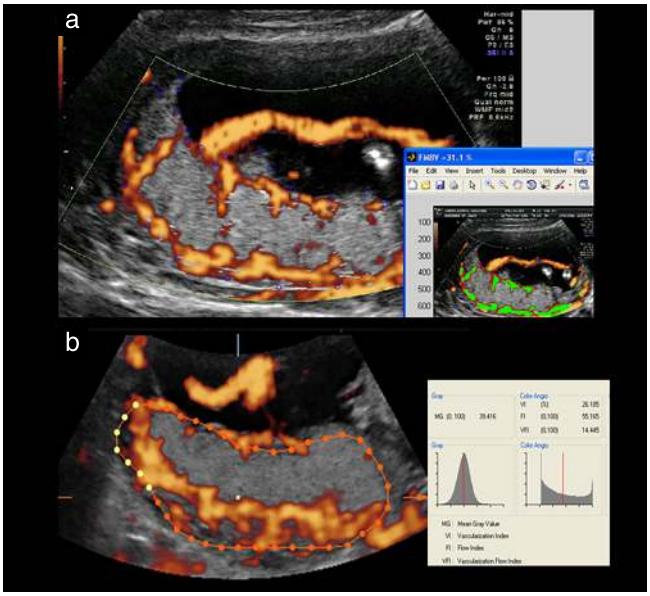

Figure 22 (a) Estimation of placental blood perfusion using power Doppler ultrasound and fractional moving blood volume, which is the fraction of the placental image occupied by blood movement (31% in this case). (b) Three-dimensional power Doppler perfusion analysis, including estimation of vascularization index (VI), flow index (FI) and vascularization flow index (VFI). VI (26.1 in this case) is the fraction of the placental volume occupied by blood movement.

Differences in uteroplacental blood perfusion between twins were reported in 64 pregnant women with a MCDA twin pregnancy complicated by selective fetal growth restriction[135]. The authors showed reduced 3D power Doppler indices in the placental region of the smaller cotwin as compared with the normally grown twin (Figure 22). Similar differences were observed in MCDA twins with discrepancy in size despite not meeting the criteria for selective fetal growth restriction. The authors also reported significant intertwin differences in umbilical artery PI; however, the difference was larger in cases with selective fetal growth restriction.

CONCLUSIONS

Doppler modalities can contribute to the diagnosis of different placental anomalies. Highly sensitive power Doppler techniques can delineate the placental functional unit as a rich component of fetal vessels surrounding a spiral artery. The number of placental functional units may be associated with obstetric complications, such as fetal growth restriction. Power Doppler and directional power Doppler can provide information on decidual vessels and blood movement. Abnormal decidual circulation increases the risk of placenta accreta. Doppler evaluation of the placenta can greatly contribute to the diagnosis and clinical management of placenta accreta, vasa previa, placental infarcts, infarction hematoma, MPFD/MFI and placental tumors. Doppler evaluation of the placenta has a limited contribution to the diagnosis and clinical management of placental abruption, placental hematomas and placental mesenchymal dysplasia, as well as assessment of anastomoses in monochorionic twins.

ACKNOWLEDGMENT

We are profoundly grateful to Professor Roberto Romero and the Perinatology Research Branch (Division of Obstetrics and Maternal–Fetal Medicine, Division of Intramural Research, *Eunice Kennedy Shriver* National Institute of Child Health and Human Development, National Institutes of Health, U.S. Department of Health and Human Services (NICHD/NIH/DHHS)), for allowing us to include several placental images which were obtained while the first author (E.H.-A.) worked at the Perinatology Research Branch.

REFERENCES

1. Konje JC, Kaufmann P, Bell SC, Taylor DJ. A longitudinal study of quantitative uterine blood flow with the use of color power angiography in appropriate for gestational age pregnancies. *Am J Obstet Gynecol* 2001; **185**: 608–613.
2. Thaler I, Manor D, Itskovitz J, Rottem S, Levit N, Timor-Tritsch I, Brandes JM. Changes in uterine blood flow during human pregnancy. *Am J Obstet Gynecol* 1990; **162**: 121–125.
3. Issa B, Moore RJ, Bowtell RW, Baker PN, Johnson IR, Worthington BS, Gowland PA. Quantification of blood velocity and flow rates in the uterine vessels using echo planar imaging at 0.5 Tesla. *J Magn Reson Imaging* 2010; **31**: 921–927.
4. Collins SL, Stevenson GN, Noble JA, Impey L. Developmental changes in spiral artery blood flow in the human placenta observed with colour Doppler ultrasonography. *Placenta* 2012; **33**: 782–787.
5. Jurkovic D, Jauniaux E, Kurjak A, Hustin J, Campbell S, Nicolaides KH. Transvaginal color Doppler assessment of the uteroplacental circulation in early pregnancy. *Obstet Gynecol* 1991; **77**: 365–369.
6. Stevenson GN, Noble JA, Welsh AW, Impey L, Collins SL. Automated Visualization and Quantification of Spiral Artery Blood Flow Entering the First-Trimester Placenta, Using 3-D Power Doppler Ultrasound. *Ultrasound Med Biol* 2018; **44**: 522–531.
7. Schiffer V, Evers L, de Haas S, Ghossein-Doha C, Al-Nasiry S, Spaanderman M. Spiral artery blood flow during pregnancy: a systematic review and meta-analysis. *BMC Pregnancy Childbirth* 2020; **20**: 680.
8. Odibo AO, Kayisli U, Lu Y, Kayisli O, Schatz F, Odibo L, Chen H, Bronsteen R, Lockwood CJ. Longitudinal assessment of spiral artery and intravillous arteriole blood flow and adverse pregnancy outcome. *Ultrasound Obstet Gynecol* 2022; **59**: 350–357.
9. Orden MR, Gudmundsson S, Kirkinen P. Intravascular ultrasound contrast agent: an aid in imaging intervillous blood flow? *Placenta* 1999; **20**: 235–240.
10. Wang LL, Liu H, Zhao SJ, Shen L, Xie T, Luo J, Mor G, Liao AH. The metabolic landscape of decidua in recurrent pregnancy loss using a global metabolomics approach. *Placenta* 2021; **112**: 45–53.
11. O'Hern Perfetto C, Fan X, Dahl S, Krieg S, Westphal LM, Bunker Lathi R, Nayak NR. Expression of interleukin-22 in decidua of patients with early pregnancy and unexplained recurrent pregnancy loss. *J Assist Reprod Genet* 2015; **32**: 977–984.
12. Hannon T, Innes BA, Lash GE, Bulmer JN, Robson SC. Effects of local decidua on trophoblast invasion and spiral artery remodeling in focal placenta creta – an immunohistochemical study. *Placenta* 2012; **33**: 998–1004.
13. Horinouchi T, Yoshizato T, Kojiro-Sanada S, Kozuma Y, Yokomine M, Ushijima K. Missing decidual Doppler signals as a new diagnostic criterion for placenta accreta spectrum: A case described using superb microvascular imaging. *J Obstet Gynaecol Res* 2021; **47**: 411–415.
14. Carlson BM. Placenta and Extraembryonic Membranes. In *Human Embryology and Developmental Biology* (5th edn), Carlson BM (ed). Elsevier: St Louis, MO, 2014; 117–135.
15. Benirschke K, Kaufmann P, Baergen RN. *Pathology of the Human Placenta* (5th edn). Springer-Verlag: New York, NY, USA, 2006.
16. Moore KL, Persaud TVN, Torchia MG. *The developing human: Clinically oriented embryology* (8th edn). Saunders Elsevier: Philadelphia, PA, USA, 2008.
17. Cho FN, Liu CB, Li JY, Yu KJ, Chen SN. Prominent decidual vasculature overlying the internal cervical os: an entity potentially leading to acute life-threatening antepartum hemorrhage. *J Chin Med Assoc* 2010; **73**: 216–218.
18. Peker T, Omeroglu S, Hamdemir S, Celik H, Tatar I, Aksakal N, Turgut HB. Three-dimensional assessment of the morphology of the umbilical artery in normal and pre-eclamptic placentas. *J Obstet Gynaecol Res* 2006; **32**: 468–474.
19. Mu J, Kanzaki T, Tomimatsu T, Fukuda H, Fujii E, Takeuchi H, Murata Y. Investigation of intraplacental villous arteries by Doppler flow imaging in growth-restricted fetuses. *Am J Obstet Gynecol* 2002; **186**: 297–302.
20. Lacin S, Demir N, Koyuncu F, Goktay Y. Value of intraplacental villous artery Doppler measurements in severe preeclampsia. *J Postgrad Med* 1996; **42**: 101–104.
21. Jaffe R, Woods JR. Doppler velocimetry of intraplacental fetal vessels in the second trimester: improving the prediction of pregnancy complications in high-risk patients. *Ultrasound Obstet Gynecol* 1996; **8**: 262–266.
22. Babic I, Ferraro ZM, Garbedian K, Oulette A, Ball CG, Moretti F, Gruslin A. Intraplacental villous artery resistance indices and identification of placenta-mediated diseases. *J Perinatol* 2015; **35**: 793–798.
23. Collins SL, Welsh AW, Impey L, Noble JA, Stevenson GN. 3D fractional moving blood volume (3D-FMBV) demonstrates decreased first trimester placental vascularity in pre-eclampsia but not the term, small for gestation age baby. *PLoS One* 2017; **12**: e0178675.
24. Higgins LE, Heazell AEP, Simcox LE, Johnstone ED. Intra-placental arterial Doppler: A marker of fetoplacental vascularity in late-onset placental disease? *Acta Obstet Gynecol Scand* 2020; **99**: 865–874.
25. Karttunen V, Sahlman H, Repo JK, Woo CS, Myohanen K, Myllynen P, Vahakangas KH. Criteria and challenges of the human placental perfusion – Data from a large series of perfusions. *Toxicol In Vitro* 2015; **29**: 1482–1491.
26. Panigel M, Pascaud M, Brun JL. [Radioangiographic study of circulation in the villi and intervillous space of isolated human placental cotyledon kept viable by perfusion]. *J Physiol (Paris)* 1967; **59**: 277.
27. Mandelbrot L, Ceccaldi PF, Duro D, Le M, Pencole L, Peytavin G. Placental transfer and tissue accumulation of dolutegravir in the ex vivo human cotyledon perfusion model. *PLoS One* 2019; **14**: e0220323.
28. Hutson JR, Garcia-Bournissen F, Davis A, Koren G. The human placental perfusion model: a systematic review and development of a model to predict in vivo transfer of therapeutic drugs. *Clin Pharmacol Ther* 2011; **90**: 67–76.
29. Sun L, Li N, Jia L, Zhang C, Wang S, Jiao R, Wang L, Ye Y. Comparison of Superb Microvascular Imaging and Conventional Doppler Imaging Techniques for Evaluating Placental Microcirculation: A Prospective Study. *Med Sci Monit* 2020; **26**: e926215.
30. Chen X, Wei X, Zhao S, Huang H, Wang W, Qiu J, Chen X, Cheng C, Tian Z, Rychik J. Characterization of Placental Microvascular Architecture by MV-Flow Imaging in Normal and Fetal Growth-Restricted Pregnancies. *J Ultrasound Med* 2021; **40**: 1533–1542.
31. Rizzo G, Pietrolucci ME, Aiello E, Dijmeli E, Bosi C, Arduini D. Are there any differences in three-dimensional placental vascular indices obtained using conventional power Doppler and high-definition flow imaging? *J Matern Fetal Neonatal Med* 2012; **25**: 1664–1667.
32. Berkley EM, Abuhamad AZ. Prenatal diagnosis of placenta accreta: is sonography all we need? *J Ultrasound Med* 2013; **32**: 1345–1350.
33. D'Antonio F, Iacovella C, Bhide A. Prenatal identification of invasive placentation using ultrasound: systematic review and meta-analysis. *Ultrasound Obstet Gynecol* 2013; **42**: 509–517.
34. D'Antonio F, Bhide A. Ultrasound in placental disorders. *Best Pract Res Clin Obstet Gynaecol* 2014; **28**: 429–442.
35. Melcer Y, Jauniaux E, Maymon S, Tsviban A, Pekar-Zlotin M, Betser M, Maymon R. Impact of targeted scanning protocols on perinatal outcomes in pregnancies at risk of placenta accreta spectrum or vasa previa. *Am J Obstet Gynecol* 2018; **218**: 443.e1–443.e8.
36. Jauniaux E, Collins S, Burton GJ. Placenta accreta spectrum: pathophysiology and evidence-based anatomy for prenatal ultrasound imaging. *Am J Obstet Gynecol* 2018; **218**: 75–87.
37. Zosmer N, Jauniaux E, Bunce C, Panaiotova J, Shaikh H, Nicholaides KH. Interobserver agreement on standardized ultrasound and histopathologic signs for the prenatal diagnosis of placenta accreta spectrum disorders. *Int J Gynaecol Obstet* 2018; **140**: 326–331.
38. Jauniaux E, Jurkovic D. Placenta accreta: pathogenesis of a 20th century iatrogenic uterine disease. *Placenta* 2012; **33**: 244–251.
39. Bowman ZS, Eller AG, Kennedy AM, Richards DS, Winter TC 3rd, Woodward PJ, Silver RM. Accuracy of ultrasound for the prediction of placenta accreta. *Am J Obstet Gynecol* 2014; **211**: 177.e1–7.
40. Coutinho CM, Giorgione V, Noel L, Liu B, Chandraharan E, Pryce J, Frick AP, Thilaganathan B, Bhide A. Effectiveness of contingent screening for placenta accreta spectrum disorders based on persistent low-lying placenta and previous uterine surgery. *Ultrasound Obstet Gynecol* 2021; **57**: 91–96.
41. Skupski DW, Duzyj CM, Scholl J, Perez-Delboy A, Ruhstaller K, Plante LA, Hart LA, Palomares KTS, Ajemian B, Rosen T, Kinzler WL, Ananth C, Perinatal Research Consortium. Evaluation of classic and novel ultrasound signs of placenta accreta spectrum. *Ultrasound Obstet Gynecol* 2022; **59**: 465–473.
42. Pilloni E, Alemanno MG, Gaglioti P, Sciarrone A, Garofalo A, Biolcati M, Botta G, Viora E, Todros T. Accuracy of ultrasound in antenatal diagnosis of placental attachment disorders. *Ultrasound Obstet Gynecol* 2016; **47**: 302–307.
43. Jauniaux E, Moffett A, Burton GJ. Placental Implantation Disorders. *Obstet Gynecol Clin North Am* 2020; **47**: 117–132.
44. Berkley EM, Abuhamad A. Imaging of Placenta Accreta Spectrum. *Clin Obstet Gynecol* 2018; **61**: 755–765.
45. Zhang J, Li H, Wang F, Qin H, Qin Q. Prenatal Diagnosis of Abnormal Invasive Placenta by Ultrasound: Measurement of Highest Peak Systolic Velocity of Subplacental Blood Flow. *Ultrasound Med Biol* 2018; **44**: 1672–1678.
46. Cali G, Giambanco L, Puccio G, Forlani F. Morbidly adherent placenta: evaluation of ultrasound diagnostic criteria and differentiation of placenta accreta from percreta. *Ultrasound Obstet Gynecol* 2013; **41**: 406–412.
47. Collins SL, Stevenson GN, Al-Khan A, Illsley NP, Impey L, Pappas L, Zamudio S. Three-Dimensional Power Doppler Ultrasonography for Diagnosing Abnormally Invasive Placenta and Quantifying the Risk. *Obstet Gynecol* 2015; **126**: 645–653.
48. Haidar ZA, Papanna R, Sibai BM, Tatevian N, Viteri OA, Vowels PC, Blackwell SC, Moise KJ Jr. Can 3-dimensional power Doppler indices improve the prenatal diagnosis of a potentially morbidly adherent placenta in patients with placenta previa? *Am J Obstet Gynecol* 2017; **217**: 202.e1–202.e13.
49. Shih J-C, Kang J, Tsai S-J, Lee J-K, Liu K-L, Huang K-Y. The "rail sign": an ultrasound finding in placenta accreta spectrum indicating deep villous invasion and adverse outcomes. *Am J Obstet Gynecol* 2021; **225**: 292.e1–292.e17.
50. di Pasquo E, Ghi T, Cali G, D'Antonio F, Fratelli N, Forlani F, Prefumo F, Kaihura CT, Volpe N, Dall'Asta A, Frusca T. Intracervical lakes as sonographic marker of placenta accreta spectrum disorder in patients with placenta previa or low-lying placenta. *Ultrasound Obstet Gynecol* 2020; **55**: 460–466.
51. Cali G, Forlani F, Lees C, Timor-Tritsch I, Palacios-Jaraquemada J, Dall'Asta A, Bhide A, Flacco ME, Manzoli L, Labate F, Perino A, Scambia G, D'Antonio F. Prenatal ultrasound staging system for placenta accreta spectrum disorders. *Ultrasound Obstet Gynecol* 2019; **53**: 752–760.
52. Zhang W, Geris S, Al-Emara N, Ramadan G, Sotiriadis A, Akolekar R. Perinatal outcome of pregnancies with prenatal diagnosis of vasa previa: systematic review and meta-analysis. *Ultrasound Obstet Gynecol* 2021; **57**: 710–719.
53. Ruiter L, Kok N, Limpens J, Derks JB, de Graaf IM, Mol BW, Pajkrt E. Systematic review of accuracy of ultrasound in the diagnosis of vasa previa. *Ultrasound Obstet Gynecol* 2015; **45**: 516–522.
54. Ochiai D, Endo T, Oishi M, Kasuga Y, Ikenoue S, Tanaka M. Vasa previa with fetal vessels running transversely across the cervix: a diagnostic pitfall. *Ultrasound Obstet Gynecol* 2021; **58**: 485–486.
55. Ranzini AC, Oyelese Y. How to screen for vasa previa. *Ultrasound Obstet Gynecol* 2021; **57**: 720–725.
56. Hayata E, Nakata M, Oji A, Takano M, Nagasaki S, Morita M. Sonographic diagnosis of vasa previa using four-dimensional spatiotemporal image correlation. *Ultrasound Obstet Gynecol* 2019; **53**: 701–702.
57. Zhang W, Geris S, Beta J, Ramadan G, Nicolaides KH, Akolekar R. Prevention of stillbirth: impact of two-stage screening for vasa previa. *Ultrasound Obstet Gynecol* 2020; **55**: 605–612.

58. Kulkarni A, Powel J, Aziz M, Shah L, Lashley S, Benito C, Oyelese Y. Vasa Previa: Prenatal Diagnosis and Outcomes: Thirty-five Cases From a Single Maternal–Fetal Medicine Practice. *J Ultrasound Med* 2018; **37**: 1017–1024.
59. Sutera M, Garofalo A, Pilloni E, Parisi S, Alemanno MG, Menato G, Sciarrone A, Viora E. Vasa previa: when antenatal diagnosis can change fetal prognosis. *J Perinat Med* 2021; **49**: 915–922.
60. Lo A, Berman S, Chaiworapongsa T, Asaad R, Gonik B. Vasa previa with pulsed-wave Doppler depicting maternal heart rate. *Ultrasound Obstet Gynecol* 2020; **56**: 460–461.
61. Aoki M, Obata S, Odagami M, Miyagi E, Aoki S. Prenatal diagnosis of vasa previa and the course of the cord vessels contribute to the safety of Cesarean sections: A case report. *Clin Case Rep* 2019; **7**: 2114–2117.
62. Jauniaux E, Alfirevic Z, Bhide AG, Burton GJ, Collins SL, Silver R, Royal College of Obstetricians and Gynaecologists. Vasa Praevia: Diagnosis and Management: Green-top Guideline No. 27b. *BJOG* 2019; **126**: e49–e61.
63. Gomes A, Rezende J, Vogt MF, Zaconeta A. Vasa Previa: A Cautious Approach at Caesarean Section. *J Obstet Gynaecol Can* 2017; **39**: 203–204.
64. Hwang HS, Sohn IS, Kwon HS. The clinical significance of large placental lakes. *Eur J Obstet Gynecol Reprod Biol* 2012; **162**: 139–143.
65. Reis NS, Brizot ML, Schultz R, Nomura RM, Zugaib M. Placental lakes on sonographic examination: correlation with obstetric outcome and pathologic findings. *J Clin Ultrasound* 2005; **33**: 67–71.
66. Wan Masliza WD, Bajuri MY, Hassan MR, Naim NM, Shuhaila A, Das S. Sonographically abnormal placenta: an association with an increased risk poor pregnancy outcomes. *Clin Ter* 2017; **168**: e283–e289.
67. Jauniaux E, Nicolaides KH. Placental lakes, absent umbilical artery diastolic flow and poor fetal growth in early pregnancy. *Ultrasound Obstet Gynecol* 1996; **7**: 141–144.
68. Moldenhauer JS, Stanek J, Warshak C, Khoury J, Sibai B. The frequency and severity of placental findings in women with preeclampsia are gestational age dependent. *Am J Obstet Gynecol* 2003; **189**: 1173–1177.
69. Vinnars MT, Nasiell J, Ghazi S, Westgren M, Papadogiannakis N. The severity of clinical manifestations in preeclampsia correlates with the amount of placental infarction. *Acta Obstet Gynecol Scand* 2011; **90**: 19–25.
70. Viero S, Chaddha V, Alkazaleh F, Simchen MJ, Malik A, Kelly E, Windrim R, Kingdom JCP. Prognostic value of placental ultrasound in pregnancies complicated by absent end-diastolic flow velocity in the umbilical arteries. *Placenta* 2004; **25**: 735–741.
71. Brosens I, Pijnenborg R, Vercruysse L, Romero R. The "Great Obstetrical Syndromes" are associated with disorders of deep placentation. *Am J Obstet Gynecol* 2011; **204**: 193–201.
72. Wallenburg HC, Stolte LA, Janssens J. The pathogenesis of placental infarction. I. A morphologic study in the human placenta. *Am J Obstet Gynecol* 1973; **116**: 835–840.
73. Fitzgerald B, Shannon P, Kingdom J, Keating S. Rounded intraplacental haematomas due to decidual vasculopathy have a distinctive morphology. *J Clin Pathol* 2011; **64**: 729–732.
74. Bendon RW. Nosology: infarction hematoma, a placental infarction encasing a hematoma. *Hum Pathol* 2012; **43**: 761–763.
75. Aurioles-Garibay A, Hernandez-Andrade E, Romero R, Qureshi F, Ahn H, Jacques SM, Garcia M, Yeo L, Hassan SS. Prenatal diagnosis of a placental infarction hematoma associated with fetal growth restriction, preeclampsia and fetal death: clinicopathological correlation. *Fetal Diagn Ther* 2014; **36**: 154–161.
76. Neville G, Russell N, O'Donoghue K, Fitzgerald B. Rounded intraplacental hematoma – A high risk placental lesion as illustrated by a prospective study of 26 consecutive cases. *Placenta* 2019; **81**: 18–24.
77. Hasegawa J, Suzuki N. SMI for imaging of placental infarction. *Placenta* 2016; **47**: 96–98.
78. Hung NA, Jackson C, Nicholson M, Highton J. Pregnancy-related polymyositis and massive perivillous fibrin deposition in the placenta: are they pathogenetically related? *Arthritis Rheum* 2006; **55**: 154–156.
79. Baergen R. *Manual of Benirschke and Kaufmann's pathology of the human placenta* (2nd edn). Springer: New York, NY, USA, 2005.
80. Faye-Petersen OM, Heller DS, Joshi VV. *Handbook of placental pathology*. Taylor & Francis: Oxford, UK, 2006.
81. Fox H. *Pathology of the placenta*. W B Saunders: London, UK, 1978.
82. Frank HG, Malekzadeh F, Kertschanska S, Crescimanno C, Castellucci M, Lang I, Desoye G, Kaufmann P. Immunohistochemistry of two different types of placental fibrinoid. *Acta Anat (Basel)* 1994; **150**: 55–68.
83. Katzman PJ, Genest DR. Maternal floor infarction and massive perivillous fibrin deposition: histological definitions, association with intrauterine fetal growth restriction, and risk of recurrence. *Pediatr Dev Pathol* 2002; **5**: 159–164.
84. Vernof KK, Benirschke K, Kephart GM, Wasmoen TL, Gleich GJ. Maternal floor infarction: relationship to X cells, major basic protein, and adverse perinatal outcome. *Am J Obstet Gynecol* 1992; **167**: 1355–1363.
85. Andres RL, Kuyper W, Resnik R, Piacquadio KM, Benirschke K. The association of maternal floor infarction of the placenta with adverse perinatal outcome. *Am J Obstet Gynecol* 1990; **163**: 935–938.
86. Bukowski R, Hansen NI, Pinar H, Willinger M, Reddy UM, Parker CB, Silver RM, Dudley DJ, Stoll BJ, Saade GR, Koch MA, Hogue C, Varner MW, Conway DL, Coustan D, Goldenberg RL, Eunice Kennedy Shriver National Institute of Child Health and Human Development (NICHD) Stillbirth Collaborative Research Network (SCRN). Altered fetal growth, placental abnormalities, and stillbirth. *PLoS One* 2017; **12**: e0182874.
87. Jindal P, Regan L, Fourkala EO, Rai R, Moore G, Goldin RD, Sebire NJ. Placental pathology of recurrent spontaneous abortion: the role of histopathological examination of products of conception in routine clinical practice: a mini review. *Hum Reprod* 2007; **22**: 313–316.
88. Spinillo A, Gardella B, Muscettola G, Cesari S, Fiandrino G, Tzialla C. The impact of placental massive perivillous fibrin deposition on neonatal outcome in pregnancies complicated by fetal growth restriction. *Placenta* 2019; **87**: 46–52.
89. Proctor LK, Whittle WL, Keating S, Viero S, Kingdom JC. Pathologic basis of echogenic cystic lesions in the human placenta: role of ultrasound-guided wire localization. *Placenta* 2010; **31**: 1111–1115.
90. Wallenburg HC. Chorioangioma of the placenta. Thirteen new cases and a review of the literature from 1939 to 1970 with special reference to the clinical complications. *Obstet Gynecol Surv* **1971**; 26: 411–425.
91. Sepulveda W, Aviles G, Carstens E, Corral E, Perez N. Prenatal diagnosis of solid placental masses: the value of color flow imaging. *Ultrasound Obstet Gynecol* 2000; **16**: 554–558.
92. Sepulveda W, Alcalde JL, Schnapp C, Bravo M. Perinatal outcome after prenatal diagnosis of placental chorioangioma. *Obstet Gynecol* 2003; **102**: 1028–1033.
93. Zanardini C, Papageorghiou A, Bhide A, Thilaganathan B. Giant placental chorioangioma: natural history and pregnancy outcome. *Ultrasound Obstet Gynecol* 2010; **35**: 332–336.
94. Ropacka-Lesiak M, Gruca-Stryjak K, Breborowicz G. Nontrophoblastic placental tumors. *Neuro Endocrinol Lett* 2012; **33**: 375–379.
95. Jauniaux E, Ogle R. Color Doppler imaging in the diagnosis and management of chorioangiomas. *Ultrasound Obstet Gynecol* 2000; **15**: 463–467.
96. Zalel Y, Weisz B, Gamzu R, Schiff E, Shalmon B, Achiron R. Chorioangiomas of the placenta: sonographic and Doppler flow characteristics. *J Ultrasound Med* 2002; **21**: 909–913.
97. Williams VL, Williams RA. Placental teratoma: prenatal ultrasonographic diagnosis. *J Ultrasound Med* 1994; **13**: 587–589.
98. Ahmed N, Kale V, Thakkar H, Hanchate V, Dhargalkar P. Sonographic diagnosis of placental teratoma. *J Clin Ultrasound* 2004; **32**: 98–101.
99. Seckl MJ, Sebire NJ, Berkowitz RS. Gestational trophoblastic disease. *Lancet* 2010; **376**: 717–729.
100. Shanbhogue AK, Lalwani N, Menias CO. Gestational trophoblastic disease. *Radiol Clin North Am* 2013; **51**: 1023–1034.
101. Huang CY, Chen CA, Hsieh CY, Cheng WF. Intracerebral hemorrhage as initial presentation of gestational choriocarcinoma: a case report and literature review. *Int J Gynecol Cancer* 2007; **17**: 1166–1171.
102. Guvendag Guven ES, Guven S, Esinler I, Ayhan A, Kucukali T, Usubutun A. Placental site trophoblastic tumor in a patient with brain and lung metastases. *Int J Gynecol Cancer* 2004; **14**: 558–563.
103. Sebire NJ, Jauniaux E. Fetal and placental malignancies: prenatal diagnosis and management. *Ultrasound Obstet Gynecol* 2009; **33**: 235–244.
104. Savelli L, Pollastri P, Mabrouk M, Seracchioli R, Venturoli S. Placental site trophoblastic tumor diagnosed on transvaginal sonography. *Ultrasound Obstet Gynecol* 2009; **34**: 235–236.
105. Boisrame T, Sananes N, Fritz G, Boudier E, Aissi G, Favre R, Langer B. Placental abruption: risk factors, management and maternal–fetal prognosis. Cohort study over 10 years. *Eur J Obstet Gynecol Reprod Biol* 2014; **179**: 100–104.
106. Fadl SA, Linnau KF, Dighe MK. Placental abruption and hemorrhage – review of imaging appearance. *Emerg Radiol* 2019; **26**: 87–97.
107. Nyberg DA, Cyr DR, Mack LA, Wilson DA, Shuman WP. Sonographic spectrum of placental abruption. *AJR Am J Roentgenol* 1987; **148**: 161–164.
108. Oyelese Y, Ananth CV. Placental abruption. *Obstet Gynecol* 2006; **108**: 1005–1016.
109. Jha P, Melendres G, Bijan B, Ormsby E, Chu L, Li CS, McGahan J. Trauma in pregnant women: assessing detection of post-traumatic placental abruption on contrast-enhanced CT versus ultrasound. *Abdom Radiol (NY)* 2017; **42**: 1062–1067.
110. Welsh AW, Bennett PR, Fisk NM. Quantitative digital analysis of regional placental perfusion using power Doppler in placental abruption. *Ultrasound Obstet Gynecol* 2001; **17**: 203–208.
111. Windrim C, Athaide G, Gerster T, Kingdom JCP. Sonographic findings and clinical outcomes in women with massive subchorionic hematoma detected in the second trimester. *J Obstet Gynaecol Can* 2011; **33**: 475–479.
112. Satomi M, Hiraizumi Y, Suzuki S. Subchorionic haematoma distinct from the placental tissue at 39 weeks' gestation. *J Obstet Gynaecol* 2012; **32**: 304–305.
113. Deans A, Jauniaux E. Prenatal diagnosis and outcome of subamniotic hematomas. *Ultrasound Obstet Gynecol* 1998; **11**: 319–323.
114. Shukunami K, Orisaka M, Orisaka S, Nishijima K, Tajima K, Goto K, Kotsuji F. A subamniotic hematoma resembling a deflated balloon. *J Matern Fetal Neonatal Med* 2004; **16**: 373–375.
115. Miyagi M, Kinjo T, Mekaru K, Nitta H, Masamoto H, Aoki Y. Massive Subchorionic Thrombohematoma (Breus' Mole) Associated with Fetal Growth Restriction, Oligohydramnios, and Intrauterine Fetal Death. *Case Rep Obstet Gynecol* 2019; **2019**: 9510936.
116. Fung TY, To KF, Sahota DS, Chan LW, Leung TY, Lau TK. Massive subchorionic thrombohematoma: a series of 10 cases. *Acta Obstet Gynecol Scand* 2010; **89**: 1357–1361.
117. Alanjari A, Wright E, Keating S, Ryan G, Kingdom J. Prenatal diagnosis, clinical outcomes, and associated pathology in pregnancies complicated by massive subchorionic thrombohematoma (Breus' mole). *Prenat Diagn* 2013; **33**: 973–978.
118. Prapas N, Liang RI, Hunter D, Copel JA, Lu LC, Pazkash V, Mari G. Color Doppler imaging of placental masses: differential diagnosis and fetal outcome. *Ultrasound Obstet Gynecol* 2000; **16**: 559–563.
119. Khong TY, Mooney EE, Nikkels PGJ, Morgan TK, Gordijn SJ. *Pathology of the Placenta: A Practical Guide*. Springer Nature, 2019. https://doi.org/10.1007/978-3-319-97214-5.
120. Tuuli MG, Norman SM, Odibo AO, Macones GA, Cahill AG. Perinatal outcomes in women with subchorionic hematoma: a systematic review and meta-analysis. *Obstet Gynecol* 2011; **117**: 1205–1212.

121. Jauniaux E, Nicolaides KH, Hustin J. Perinatal features associated with placental mesenchymal dysplasia. *Placenta* 1997; **18**: 701–706.
122. Moscoso G, Jauniaux E, Hustin J. Placental vascular anomaly with diffuse mesenchymal stem villous hyperplasia. A new clinico-pathological entity? *Pathol Res Pract* 1991; **187**: 324–328.
123. Faye-Petersen OM, Kapur RP. Placental Mesenchymal Dysplasia. *Surg Pathol Clin* 2013; **6**: 127–151.
124. Pawoo N, Heller DS. Placental mesenchymal dysplasia. *Arch Pathol Lab Med* 2014; **138**: 1247–1249.
125. Ishikawa S, Morikawa M, Umazume T, Yamada T, Kanno H, Takakuwa E, Minakami H. Anemia in a neonate with placental mesenchymal dysplasia. *Clin Case Rep* 2016; **4**: 463–465.
126. Woo GW, Rocha FG, Gaspar-Oishi M, Bartholomew ML, Thompson KS. Placental mesenchymal dysplasia. *Am J Obstet Gynecol* 2011; **205**: e3–5.
127. Vaisbuch E, Romero R, Kusanovic JP, Erez O, Mazaki-Tovi S, Gotsch F, Kim CJ, Kim JS, Yeo L, Hassan SS. Three-dimensional sonography of placental mesenchymal dysplasia and its differential diagnosis. *J Ultrasound Med* 2009; **28**: 359–368.
128. Kuwata T, Takahashi H, Matsubara S. 'Stained-glass' sign for placental mesenchymal dysplasia. *Ultrasound Obstet Gynecol* 2014; **43**: 355.
129. Matsubara S, Kuwata T, Takahashi H, Kimura Y. Diagnosis of placental mesenchymal dysplasia: magnetic resonance imaging or color Doppler? *J Obstet Gynaecol Res* 2015; **41**: 488.
130. Colpaert RM, Ramseyer AM, Luu T, Quick CM, Frye LT, Magann EF. Diagnosis and Management of Placental Mesenchymal Disease. A Review of the Literature. *Obstet Gynecol Surv* 2019; **74**: 611–622.
131. Sau A, Weber M, Shennan AH, Maxwell D. Antenatal detection of arteriovenous anastomoses in monochorionic twin pregnancy. *Int J Gynaecol Obstet* 2008; **100**: 56–59.
132. Lewi L, Deprest J, Hecher K. The vascular anastomoses in monochorionic twin pregnancies and their clinical consequences. *Am J Obstet Gynecol* 2013; **208**: 19–30.
133. Fichera A, Mor E, Soregaroli M, Frusca T. Antenatal detection of arterio-arterial anastomoses by Doppler placental assessment in monochorionic twin pregnancies. *Fetal Diagn Ther* 2005; **20**: 519–523.
134. Gratacos E, Lewi L, Munoz B, Acosta-Rojas R, Hernandez-Andrade E, Martinez JM, Carreras E, Deprest J. A classification system for selective intrauterine growth restriction in monochorionic pregnancies according to umbilical artery Doppler flow in the smaller twin. *Ultrasound Obstet Gynecol* 2007; **30**: 28–34.
135. Zhang L, Liu X, Li J, Wang X, Huang S, Luo X, Zhang H, Wen L, Tong C, Saffery R, Yan J, Qi H, Kilby MD, Baker PN. Maternal Utero-Placental Perfusion Discordance in Monochorionic-Diamniotic Twin Pregnancies with Selective Growth Restriction Assessed by Three-Dimensional Power Doppler Ultrasound. *Med Sci Monit* 2020; **26**: e919247.

